WILEY

Bedload entrainment dynamics in a partially channelized river with mixed bedload: A case study of the Drava River, Hungary

Ervin Pirkhoffer[1] | Ákos Halmai[1] | Johanna Ficsor[2,3] (ORCID) |
Alexandra Gradwohl-Valkay[3] | Dénes Lóczy[1] (ORCID) | Ádám Nagy[4] |
Zoltán Árpád Liptay[5] | Szabolcs Czigány[1]

[1]Institute of Geography and Earth Sciences, Faculty of Sciences, University of Pécs, Pécs, Hungary

[2]Department of Regional Water Management, Faculty of Water Sciences, University of Public Service, Baja, Hungary

[3]Doctoral School of Earth Sciences, Faculty of Sciences, University of Pécs, Pécs, Hungary

[4]Department of Cultural Studies, Kodolányi János University, Székesfehérvár, Hungary

[5]Forecasting Service, General Directorate of Water Management, Budapest, Hungary

Correspondence
Johanna Ficsor, Doctoral School of Earth Sciences, Faculty of Sciences, University of Pécs, Ifjúság u. 6, H-7624 Pécs, Hungary.
Email: ficsor.johanna@uni-nke.hu

Funding information
Higher Education Institutional Excellence Program of Ministry of Human Capacities (Hungary), Grant/Award Number: 20765-3/2018/FEKUTSTRAT; University of Pécs and the Hungarian Scientific Research Fund, Grant/Award Number: GINOP-2.3.2-15-2016-00055

Abstract

The morphodynamics of alluvial rivers is controlled by the mobilization of bed material. However, the details of mobilization of mixed-texture bed materials at low flows, increasingly common due to climate change, are still unclear. The 161-km-long Hungarian alluvial reach of the Drava River, downstream of sections where flow characteristics have been heavily modified by human interference, was investigated in 2019. A monitoring campaign at cross-sections, on average 5.55 km apart, was launched to study channel morphology, bedload entrainment dynamics with regard to texture. For the survey, a sonar, an ADCP and a Helley–Smith bedload sampler mounted on a double-hull vessel was used. Our research pointed out an abrupt fining between river kms (hereafter: rkm) 175 and 170 (distance from the mouth), probably due to reduced armouring. The d_{60} fraction was found to be finer than in 2003 and 2012 for the upstream stations of Botovo and Bélavár, and showed a good correspondence with the records of the Barcs and Drávaszabolcs stations. Temporal fining and higher entrainment rate are due to (a) changing climate of the catchment, that is, diminishing flow between the monitoring dates (2003, 2012 and 2019); (b) reduced armouring, (c) variability of cross-sectional position of sampling points and (d) the different mesh size of the bedload samplers employed. Calculations of shear velocity, Reynolds and Shields numbers indicate more dynamic sediment motion than observed by previous studies. Our reach-scale results may be relevant for the alluvial sections of other alpine and subalpine, partially channelized rivers of similar size, flow dynamics and mixed bedload.

KEYWORDS
armouring, bedload entrainment, bedload texture, Drava River, hydromorphology, regulated river

1 | INTRODUCTION

Bedload transport, in general, is one of the fundamental factors in fluvial hydrology, river ecology and a major concern for river engineering (Rhoads, 2020). The history of approaches to bedload transport calculations has been overviewed recently by Ancey (2020), where the mean transport rate is usually related to hydraulic conditions (water discharge, bottom shear stress or stream power). According to Sharma, Herrera-Granados, and Kumar (2019), bedload transport is additionally influenced by flow velocity and flow depth. As bed material often displays a polydisperse texture, the prediction of bedload texture and transport rate in a particular river is often challenging (Ashworth & Ferguson, 1989).

Climate change affects sediment transport (the spatial distribution of bedload fractions) indirectly through water flow, modifying physical, chemical and biological properties of the riverbed. In the future reduced runoff generation in the summer could lead to lower bedload yields in alpine rivers, but local factors can significantly modify this trend (Raymond Pralong, Turowski, Rickenmann, & Zappa, 2015). The hydrological impacts of global climate change have been described from the Drava drainage basin too. Although annual precipitation totals increased in some alpine catchments of the river, no major flood was recorded on the Drava between 1998 and 2013 (Lóczy, Dezső, & Gyenizse, 2017; Petrić, Tamás, & Lóczy, 2019). As far as the seasonal regime is concerned, the early summer flood stages of the Drava and its tributaries tend to fall, while in autumn water levels are becoming somewhat higher (Prettenthaler & Dalla-Via, 2007).

Entrainment thresholds of individual grains have been studied by numerous researchers after Einstein (1950). Bed material mobilization is largely controlled by the rate at which particles of different grain sizes are entrained from the riverbed and incorporated into the bedload (Vázquez-Tarrío, Fernández-Iglesias, Fernández García, & Marquínez, 2019). Charru, Mouilleron, and Eiff (2004) claim that the rate of entrainment depends on the Shields number. Analyses of mixed bedload movement are challenging because of the complexity of influencing factors (Ashworth & Ferguson, 1989): river competence (maximum and mean bedload diameter) and the cross-sectional distribution of size-selective transport rates. Ancey, Davison, Böhm, Jodeau, and Frey (2008) introduced two entrainment parameters into their equation, which considers the erosive action of the stream. Furbish, Ball, and Schmeeckle (2012) suggest a probabilistic description of bedload transport.

Riverbed armouring is considered to be an important control of sediment transport (Pitlick, Mueller, Segura, Cress, & Torizzo, 2008). Even a persistent armor layer, however, does not prevent the mobilization of particles from the riverbed (Wilcock & DeTemple, 2005). There is an active exchange of grains between the armored riverbed and the bedload, although not all grains may be in motion. Through the shielding effect of coarse grains on the fines, armouring ensures equal particle mobility (Hicks & Gomez, 2016). Consequently, wherever the armor is disrupted, more fines are entrained from the bed. The interactions between riverbed sediment mobilization, bedload transport and armouring are quantified by the Bathurst (2007) and

Recking, Liébault, Peteuil, and Jolimet (2012) formulae, which are particularly applicable to predict the disruption threshold of the armor under low flow conditions. However, measured thresholds are usually higher than those predicted by the formulae (López, Vericat, & Batalla, 2015). In some cases, riverbed armouring is attributed to granular segregation from below (Ferdowsi, Ortiz, Houssais, & Jerolmack, 2017). Streambed fining in response to large sediment influx may indicate an inverse relationship between armouring and the rate of sediment transport (Wilcock & DeTemple, 2005). As opposed to observations at low water stages, there is no conclusive evidence on riverbed grain size changes during floods. Flume experiments confirm armor development but do not resolve the question of armor persistence in the field (Wilcock & DeTemple, 2005).

As opposed to the Austrian, Slovenian and Croatian sections of the Drava River, hydroengineering works were limited to indispensable flood-prevention interventions on the lowermost (Croatian–Hungarian) section (Petric et al., 2019), which is in a close-to-natural state. The LIFE Project "Wise water management for the conservation of riverine and floodplain habitats along the Drava River" (https://wwf.hu/wisedrava/) is aimed at the rehabilitation of the channel and floodplain environment. The spatial resolution of previous surveys did not allow a detailed reconstruction of longitudinal textural variability of bedload adjusted to flow conditions and the realistic assessment of the human impact on bedload transport along the upstream section. The ongoing LIFE Project calls for the exploration of interactions between flow velocity and bedload characteristics at a higher longitudinal resolution in the Drava channel. The specific aims of the research were:

1. the establishment of relationships between reach-scale channel morphology and bedload texture;
2. the study of spatial distribution of armouring at low-flow conditions, which will be increasingly common in the future in the wake of aridification, a major manifestation of climate change in the Lower Drava Basin;
3. the quantitative analysis of entrainment dynamics relying on calculation of reach-scale shear velocities at low flow;
4. the tracking of bedload motion and the identification of threshold shear velocities in function of flow measured by Acoustic Doppler Current Profiler (ADCP).

2 | MATERIALS AND METHODS

2.1 | Study area

The Drava River is a major right-bank tributary of the Danube. It has a total length of 725 km from its source in Northeastern Italy in the Dolomites along the southwestern border of Hungary to its confluence at Aljmaš in Croatia. It has the fourth largest mean discharge (550 m^3/s) among the rivers of Hungary (Lovász, 1974).

The largest tributary of the Drava, the Mur/Mura (catchment area: 13,800 km^2, length: 464 km, mean discharge: 166 m^3/s) is the only source of gravel-size bedload downstream of the hydropower

dams, that is, for the Hungarian reach. Average bedload input from the Mura to the Drava at Botovo (rkm 227) was 24,452 t/y over the period of 2004–2010 (Bonacci & Oskoruš, 2010).

The lower joint Hungarian–Croatian Drava section of 161 km has a significant ecological and touristic potential. The river channel and the riparian zone are supervised by the Danube-Drava National Park. Several endangered plant and animal species are found here (Purger, 2008), including the only existing population of a caddisfly species (Platyphylax frauenfeldi) (Uherkovich & Nógrádi, 1997). In addition to caddisflies, a number of other macroinvertebrates (other insect larvae, unionid mussels, aquatic snails, crayfish and others) find their habitat and resources in coarse bed materials of mixed grain size.

In spite of the intriguing environment, few scientific studies have been conducted along the Lower Drava. The Drava River is extremely dynamic in respect to flow and sediment transport. Related to the WWF LIFE project, there are some negative tendencies as far as ecological impacts are concerned. Discharge and stage levels have been decreasing along the studied incising reach of the Drava River over the past 120 years (Bonacci & Oskoruš, 2010), with impacts on the moisture dynamics of the riparian zone. Considering the expected effects of climate change and human interventions, decreasing flow trends are expected to continue in the near future (Kiss & Andrási, 2019). Decreasing flow rates and velocities affect local ecosystems through changes in the rates of sediment transport and the size distribution of transported material. The understanding of expected changes is crucial for maintaining natural conditions and ecosystem services. The quality and dynamics of transported material determines the composition and vitality of the aquatic ecosystems. Hence, any changes in the budget of the transported material, usually as a consequence of anthropogenic influences, may irreversibly affect aquatic and riparian ecosystems (Evans & Wilcox, 2014; Owens et al., 2005). The intense deposition of fine particles may completely destroy the habitat of numerous aquatic species (Murphy et al., 2017).

Similar to most rivers in Western and Central Europe, the Drava River has been regulated over the centuries by constructing a number of flood control and bedload retention structures (Petts & Wood, 1988), which affect the bedload regime. Hydroengineering interventions, such as construction of hydropower structures in Croatia induced significant morphological changes in the channel downstream (Bonacci & Oskoruš, 2010; Słowik, Dezső, Marciniak, Tóth, & Kovács, 2018). By the late 1990s the negative effects of the systematic regulation were recognized. The purely technical flood protection led to riverbed degradation and to ecological deficits. To overcome these drawbacks integrative planning tools were introduced along the upper reaches and riverbed widening proved to be effective in mitigating bed incision while restoring morphodynamic processes (Habersack, Jäger, & Hauer, 2013). Sediment budget is closely related to river regulation operations of any kind, including the installation of flow-regulating structures and hydromorphological restoration activities. These interventions enhance the resilience and adaptability of fluvial-riparian-floodplain systems (Schwarz, 2008). Understanding the correlation between river hydraulics and sediment parameters at various flow conditions is essential (Tamás & Ficsor, 2018). Similarly, data on alluvial deposits is also indispensable for channel and riverine infrastructural management (Holmes, 2010).

Due to the temporal and spatial variability of flow characteristics, particle trajectories, sediment dispersion and channel morphology have been profoundly changed (Bialik, Nikora, Karpiński, & Rowiński, 2015; Nikora, Habersack, Huber, & McEwan, 2002). Long-term datasets for the Drava River in Carinthia (Austria) showed a spatially variable bed instability, with reaches undergoing aggradation and others degradation. Habersack, Nachtnebel, and Laronne (2001) demonstrated that continuous bedload data are useful with respect to identifying the initiation of motion. In such a supply-limited channel, where bedload often moves over an armored layer, it is apparent that local hydraulic conditions explain only a fraction (about one third) of the variation in the weak bedload flux. The temporal variability of bedload transport is also attributed to sediment supply (Hicks & Gomez, 2016).

Previous research included an analysis of the impact of dams and reservoirs on the hydrological characteristics of the Lower Drava River (Bonacci, Tadić, & Trninić, 1992) and two monitoring campaigns in 2003 and 2012 concerning river flow and grain-size distribution of sediment load at four gauged cross-sections along the Hungarian–Croatian reach of the river (Szlávik, Sziebert, & Tamás, 2012; Tamás, 2019). A bathymetric survey using sonar technology was completed in May 2019 (Halmai et al., 2020), which enabled detailed hydrodynamic and sediment transport modeling. In order to gain information on bedload transport during low discharges, flow velocity measurements and bedload material samplings were specifically conducted under low flow conditions. This type of data enables us to gain information and experience on the hydrological consequences of ongoing climate change. Our measurements between August 21 and September 6, 2019, covered a significant portion of the Hungarian reach of the Drava from rkm 236 to rkm 75 (from Őrtilos to Drávaszabolcs—Figure 1).

2.2 | Carrier platform

Our carrier platform was a double-hulled, geometry-stabilized, widebeam, low draft, pure aluminum alloy catamaran boat with the following dimensions: $6.0 \times 1.2 \times 2.3$ m (L × H × W). At the bow, the entrance edges of the hulls were rounded backwards, toward the water line. A protruding crossbeam framework connected the two hulls of the boat. This structure allowed the installation of the sonar system on a relatively stable, meanwhile low draft carrier. With this design, our primary goal was to minimize the roll of the vessel. Due to the low draft and the backwards rounded hull, we were able to approach the riverbanks securely. The propulsion of the boat was provided by a 50 HP Yamaha outboard engine (Yamaha Corporation, Hamamatsu, Shizuoka, Japan), mounted on the center of the transom beam.

2.3 | Flow measurements

Flow, depth and sediment discharge measurements were taken using a Rio Grande 1,200 kHz Broadband ADCP (Teledynemarine, RD Instruments). The ADCP device was mounted on the portside of the
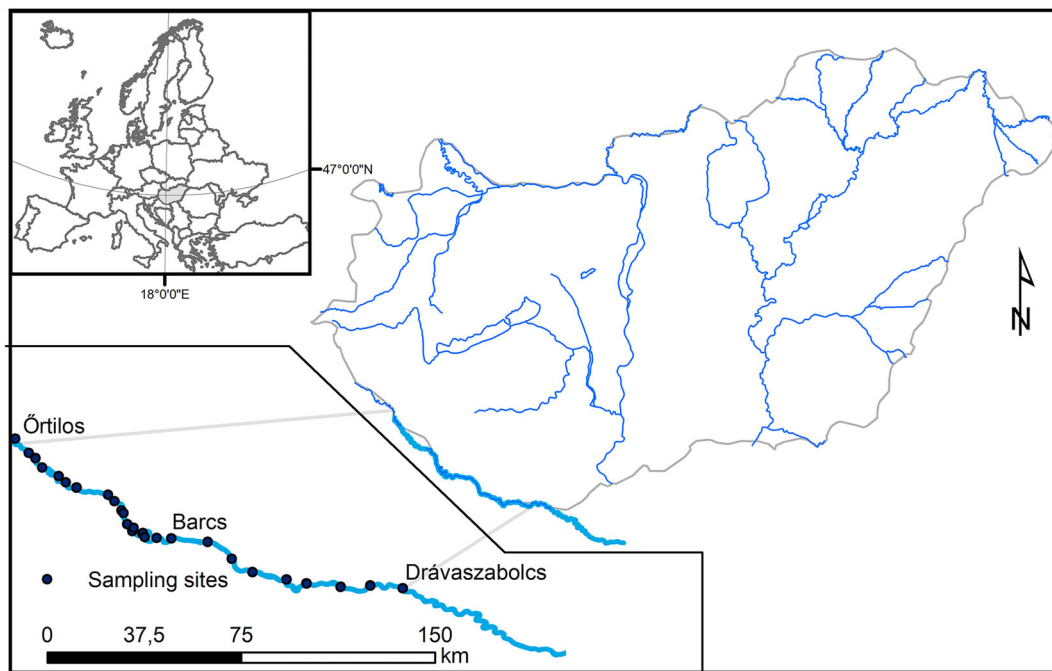
FIGURE 1 Bedload sampling locations [Color figure can be viewed at wileyonlinelibrary.com]

vessel and was connected to a GeoMax Zenith 35 Pro high-precision RTK GPS. Coordinates were obtained in a relative coordinate system in the channel compared to the riverbed and the banks and also in global projections systems. Water and sediment discharge measurements were implemented according to the Hungarian Standard ME-10-231-16: for every 5 km of the studied reach, ADCP measurements were made from the moving research vessel taking four river crossings according to the Hungarian hydrological standard protocol in every surveyed cross-section. Due to the draft of the vessel, the lower limit to ADCP measurements was set at ca. 80 cm water depth. ADCP sampling frequency ranged from 1 to 2 Hz. Discharge was variable, ranging from 210 to 400 m^3/s, but remained below the long-term average of the river over the survey period. Flow fluctuation was partly caused by the operation of the hydropower dams upstream. For each cross-section flow fields were generated in ArcGIS Pro software environment.

2.4 | Bedload sampling

Steady-boat bedload sampling (referred to a selected point in the channel bed) was carried out at 1.5 to 11 km cross-section intervals (on the average 5.55 km). Sampling points along the longitudinal profile were selected with regard to channel morphology. In the vicinity of abrupt changes in channel and flow properties, the interval of sampling was shortened to 1.5 km. Within each cross-section, we aimed at sampling at three sites: along the thalweg and on both sides of it closer to the banks.

Samples were taken with a Helley–Smith sampler. For the modified sampler the part to which the sampling bag is attached had a cuboid instead of a funnel shape. Due to surface currents, sampling locations varied in a circle of a radius of 5 m. Measurement accuracy was highly

dependent on flow velocities. Coordinates, obtained by the aforementioned RTK GPS at a spatial accuracy of 1–2 cm, were then averaged in ArcGIS to establish the exact coordinates of the verticals. Samples were taken at 3–5 verticals per cross-section, with a sampling period of 5 min. Verticals were selected based on depth profiles obtained by former sonar measurements and quasi-concurrent ADCP measurements taken right before the samplings. The bedload sampler was lowered and raised by a winch-integrated crane (Figure 2).

The modified Helley–Smith bedload sampler was equipped with a ballast of 30 kg on its top to ensure steady sampling. The sampler was also equipped with an OTT MF pro water depth and water velocity sensor 120 cm above the bottom of the sampler. The OTT MF pro was used for double checking sampling depth and the corresponding velocity. A GoPro camera was mounted on the top of the ballast on an arm of 22 cm and was used to validate the texture and movement of bedload particles. The bedload sampler was specifically adapted to the flow conditions of the Drava River, but was actually based on the description provided by Emmett (2010). The sampler had an entrance nozzle of 12 cm by 20 cm with a 46 cm long sample bag constructed of 0.1 mm mesh polyester. The sample bag had a surface area of about 1,900 cm^2. The sampler was also equipped with both a horizontal and a vertical stabilizer. The efficiency of the sampler had been calibrated using sediment rating curves (Bunte, Abt, Swingle, & Potyondy, 2010).

2.5 | Laboratory measurements of sediment texture

Bedload samples were oven-dried at 105°C for 24 hr. Sediments were dry-sieved with a sieve series 16, 8, 4, 2.8, 2, 1, 0.5 and 0.25 mm
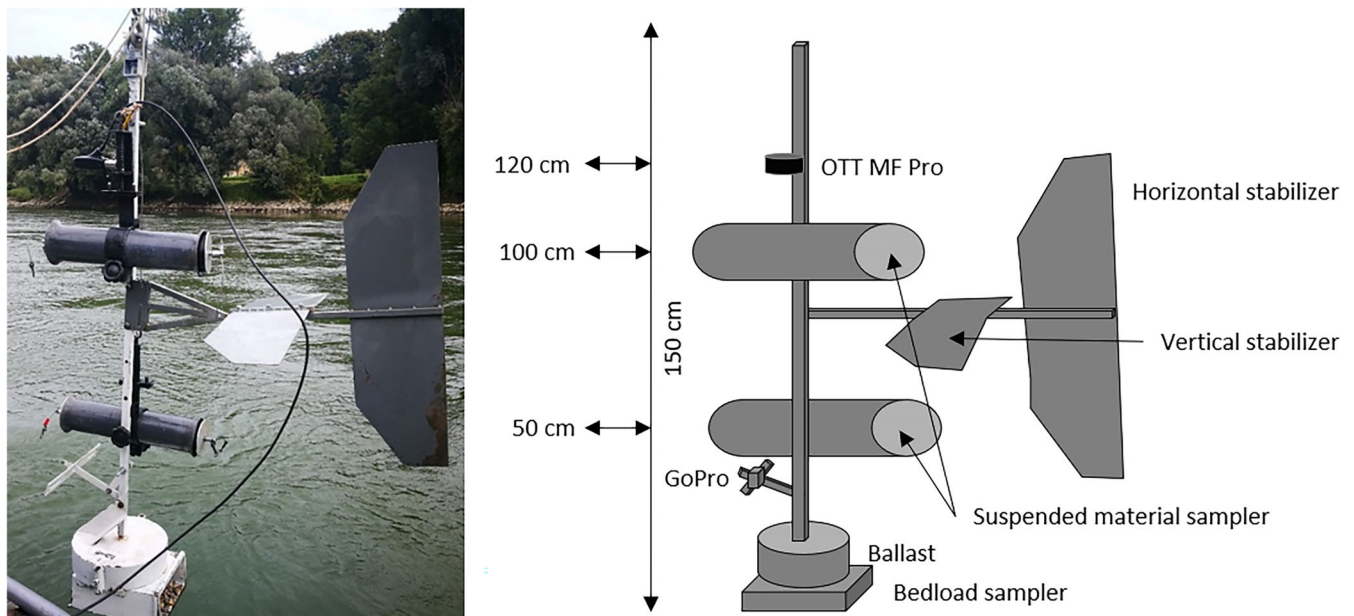
FIGURE 2 The modified Helley–Smith bedload sampler with the OTT MF Pro water velocity sensor with two suspended material sampler (shown without the sampling bag) [Color figure can be viewed at wileyonlinelibrary.com]

mesh sizes using an electronic shaker (Fritsch Analysette 3 Pro, Fritsch GmbH, Idar-Oberstein, Germany) for 2 min. Particle size distribution of the <0.25 mm fraction was determined with static light scattering technique using a Malvern 3000 (Malvern Inc., Malvern, England, UK) particle size analyzer. Sediments were chemically dispersed for organic matter and $CaCO_3$ removal, using H_2O_2 and HCl solutions, respectively.

Texture was classified in the Statistical Package for the Social Sciences (SPSS) software for 7 size classes using the centroid linkage method where the distance between the two clusters is based on the Euclidean distance. Seven textural classes, coarse gravel, coarse-medium gravel, medium-fine gravel, sandy fine gravel, gravelly coarse sand, coarse sand and medium sand textural classes were identified. Cross-sections were plotted with the integration of the ADCP data in the formerly acquired bathymetric data. Functional relationships for the data couplets of flow velocity and median particle size, obtained for each monitored verticals, were then analyzed.

2.6 | Calculation of cross-section-averaged shear velocity

The Shields number (or entrainment function) is frequently used for the characterization of the incipient motion of the bed material. Shields numbers were established using two methods. The first method, hereafter called "estimated Shields number," employed the ADCP measurements during the monitoring campaign, while the second method ("calculated Shields number") was based on the general hydraulic parameters (slope and flow depth) of the reaches immediately upstream and downstream of the transects of interest.

2.6.1 | Shields number estimation

We assumed that bottom flow velocity, which controls sediment motion, is extrapolated from the measured flow velocities in the vertical above, using the WinRiverII software of the ADCP (Teledyne, 2018). For the calculation of velocity and flow as a function of depth the software employs the flow resistance-based power formula (Power Curve Fit) presented by Chen (1991). The WinRiverII software combines this formula with the Manning equation, which is valid for open channels (Simpson & Oltmann, 1990):

$$\frac{u}{u^*} = 9.5\left(\frac{z}{z_0}\right)^b, \tag{1}$$

where u is flow velocity at a height of z above the channel bottom, u^* is shear velocity, z is the height above the channel bottom, z_0 is height of channel bottom roughness and b is a constant that has a value of 1/6.

For the calculation of u_0, the corresponding depth of z_0 was determined based on the particle size distribution of bedload. Parameter u (flow velocity) can be calculated according to the following formula:

$$u = a'z^b, \tag{2}$$

where $a' = (9.5u^*/z_0)^b$.

From the Nikuradse roughness height (k_s) z_0 can be calculated for any arbitrary height k above the channel floor (Nikuradse, 1933):

$$k_s = \left(\frac{26}{k}\right)^6 = 30z_0. \tag{3}$$

From the van Rijn assumption (van Rijn, 1984):

$$k_s = 3d_{90}. \tag{4}$$

Therefore, z_0 is calculated from the formula:

$$z_0 = \frac{d_{90}}{10}. \tag{5}$$

Shear velocity (u^*) is calculated by rearranging it into Equation (1):

$$u^* = \frac{u_0}{9,5\left(\frac{z_0}{z_0}\right)^b}. \tag{6}$$

Mean shear velocities are estimated for the entire cross-section. Reynolds numbers are calculated using the following formula:

$$Re = \frac{u^*d}{v}. \tag{7}$$

2.6.2 | Shields number calculation

Sediment transport is initiated if the Shields number, θ, is greater than the threshold value:

$$\theta = \frac{\tau}{(\rho_s - \rho)gd}, \tag{8}$$

where τ is shear stress, g is acceleration due to gravity, d is particle diameter, ρ_s is particle density and ρ is the density of water.

Although this calculation originally refers to bedload of homogeneous grain-size composition, however, we considered the results by Wan Mohtar, Junaidi, and Mukhlisin (2016), who claimed that for mixed load median grain diameter is characteristic. Therefore, we calculated with the d_{50} value of samples.

Shear stress was calculated from the following formula:

$$\tau = \rho u^{*2}. \tag{9}$$

Shear velocity u^* was calculated as follows:

$$u^* = \sqrt{ghS_f}, \tag{10}$$

where h is flow depth and S_f is slope.

Therefore, Shield number was identified as follows:

$$\theta = \frac{\rho u^{*2}}{(\rho_s - \rho)gd} = \frac{\rho h S_f}{(\rho_s - \rho)d}. \tag{11}$$

This estimation has been adapted from Sharma et al. (2019). The algorithm uses Equation (3) to calculate shear velocity u^* and

Equation (1) for the calculation of Shields number. Average water depth and the slope of the water surface were measured during our field campaign. As the measurement campaign was not carried out on consecutive days, S_f values were only available for selected transects. Hence, the Shields parameter was only calculated for the cross-sections of rkm 225, 165, 115, 105 and 75.

3 | RESULTS AND DISCUSSION

3.1 | Textural properties of bedload

Our findings revealed that overall bedload fining in the Drava follows a somewhat similar longitudinal pattern to other, heavily meandering rivers (e.g., Habersack et al., 2001). Generally, the riverbed indicated a great variability in bedload texture. In accordance with Tamás (2019), in terms of bedload texture, the studied reach is subdivided into two main sections. Upstream of about rkm 175, coarse and medium gravel dominated the riverbed. At about rkm 170 an abrupt decrease was found in the bed slope. Downstream of this point first fine gravel, then coarse sand prevailed (Figure 3).

A sharp contrast between gravel and sand textural classes was observed along the longitudinal profile of the Drava River (Figure 4).

At the confluence with the Mura River (at the village of Őrtilos), coarse gravel ($d > 16$ mm, 69%) dominated the bedload, transported by the Mura River from the Eastern Alps. The bedload of the Mura River is predominantly gravel. Due to the dams on its upper reaches, however, the Drava River is dominated by finer-grained sediments upstream of the Mura confluence. At the Őrtilos cross-section (at rkm 236) particles less than 2 mm in diameter were almost completely flushed out from the samples. At a distance of 225 km from the mouth, the fraction $d > 16$ mm decreased to 39% while particles larger than 8 mm accounted for more than 70% of the total sediment. Fine gravel armouring was probably responsible for the abundance of sand fraction (fine gravel mixed with coarse sand) at rkm 185. (Where the coarsest fraction did not exceed 1%, no armouring occurred.) The clear dominance of fine texture was observed downstream of 145 km from the mouth (Figure 5). The textural variability between rkms 170 and 145 is explained by the influence of river regulation as variable river competence is controlled by the position of reaches where cutoffs were recently made (Table 1).

Our results refined the picture of textural distribution of bedload along the Drava channel and hydromorphological explanations could be found. Our results indicated a similarly abrupt fining between rkms 175 and 170 but several reaches of relative coarsening downstream were also identified (Figure 4). Medium gravel reappeared at rkm 160 six kilometers upstream from Barcs. Nonetheless, we need to emphasize that samples were taken 3–5 verticals per transect, hence our results indicate maximum values for the studied cross-sections. As congruently pointed out by Tamás (2019), variability of bedload pattern can be attributed to the periodic armouring of the riverbed and the flow distributions in meanders.

FIGURE 3 Bedload textures at sharp textural boundaries in the Drava River [Color figure can be viewed at wileyonlinelibrary.com]
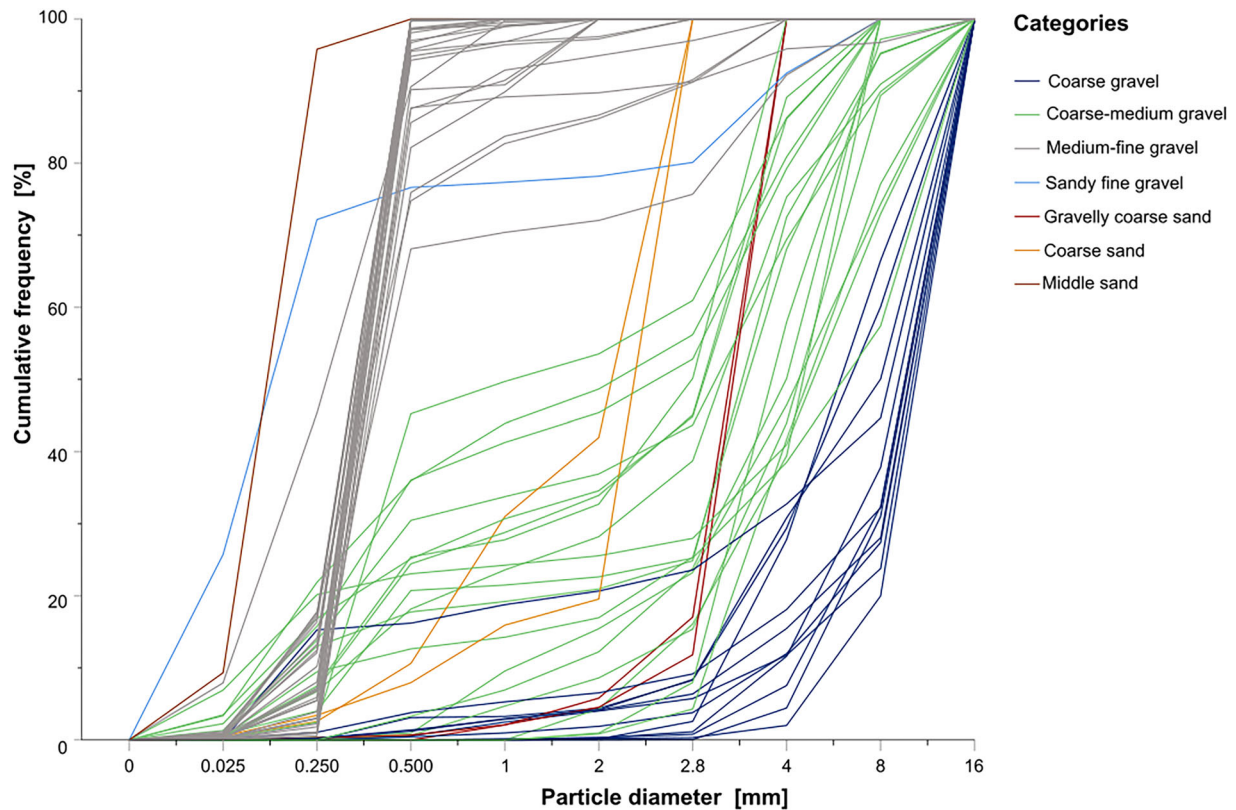
FIGURE 4 Textural categories of the 63 bedload samples using the employed hierarchical cluster analysis algorithm of the SPSS (see details in Section 2) [Color figure can be viewed at wileyonlinelibrary.com]
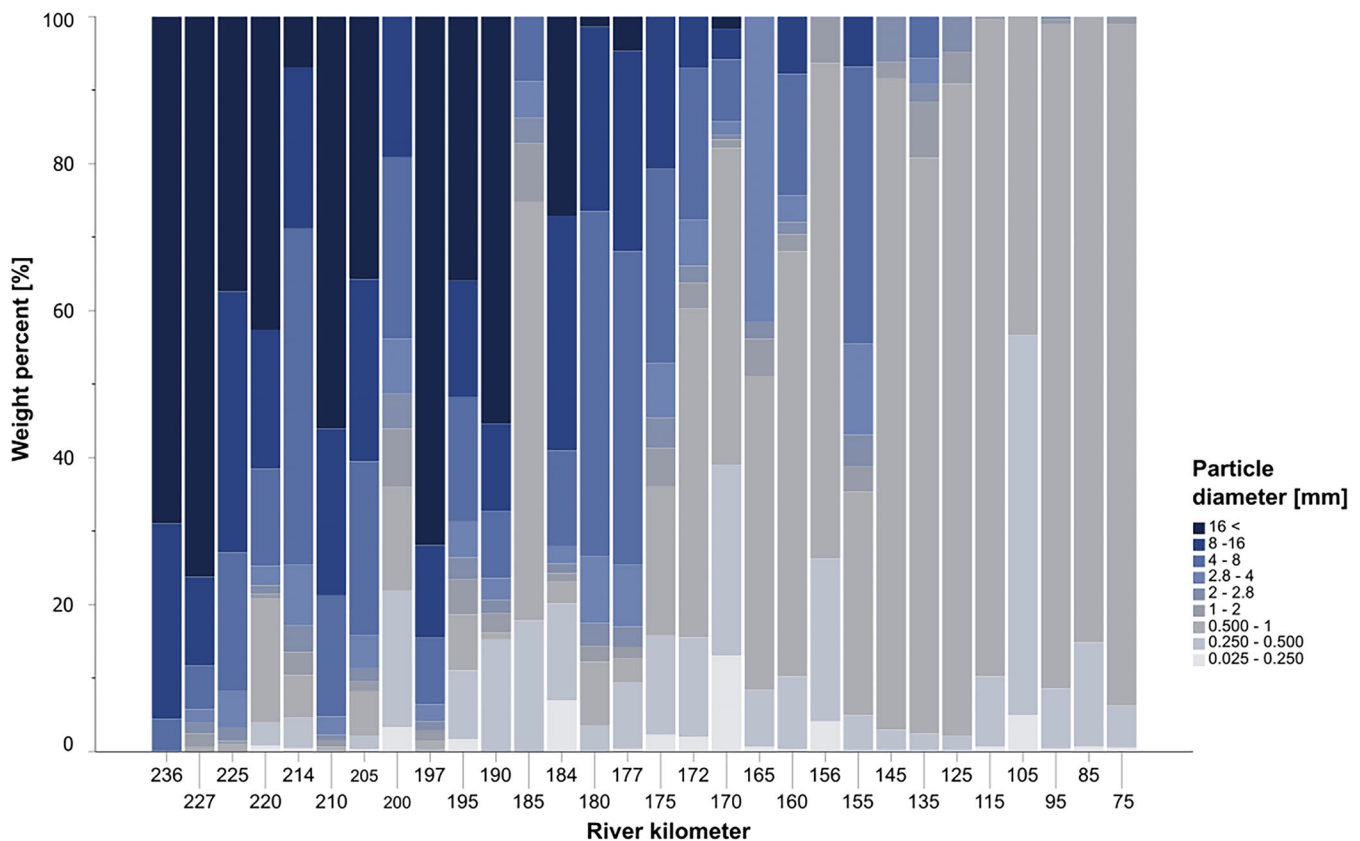
FIGURE 5 Longitudinal spatial distribution of bedload size categories of the Drava River as a function of distance from the mouth between river kms 230 and 75 [Color figure can be viewed at wileyonlinelibrary.com]

In the near future, lower-than-medium water stages may dominate river flow due to climate change, therefore, we focused our analysis on such water stages. Under such conditions, even minor differences in riverbed gradient may be influential on gravel deposition and riverbed armouring. The reappearance of gravel bedload (armouring) downstream of rkm 170 is related to increased gradients along reaches where meander cutoffs were artificially created during river regulation. The impacts of meander cutoffs in the 20th century on riverbed gradient and flow velocity are still discernible. (The last cutoff along this section happened in 1991.) There are altogether eight channel reaches which are usually still narrower than average (250 m at medium stage), created by human intervention after 1920 along the rkm 170 to 75 section, four out of which show coarsening of bed material in high percentage causing armouring (Table 1).

As far as temporal changes are concerned, our results corroborated the former findings on the spatial distribution of bedload in respect to textural properties published by Tamás (2019), who found an increase of d_{60} diameter between 2003 and 2012 in Bélavár (rkm 198.5) and Barcs (rkm 154), but revealed a slight drop at Botovo (rkm 227.5), while no significant changes could be detected at Drávaszabolcs (rkm 78) between the two dates of sampling (Figure 6a).

In the transect at Botovo, our results indicated d_{60} diameters between 5.4 and 11.8 mm with a mean of 8.1 mm, which is significantly lower than the corresponding values in 2003 (13 mm) and 2012 (12.5 mm). The mean d_{60} diameter at Bélavár was 6.74 (min.:

2.2 mm, max.: 11.6 mm) mm, compared to 7.8 and 11.9 mm in 2003 and 2012, respectively. At Barcs (rkm 155) the mean d_{60} diameter was 2.87 mm, with a minimum and maximum of 0.33 and 3.04 mm, respectively. This is higher than both the 2003 and 2012 values of 1 and 2.5 mm, respectively, but lower than the values measured at rkm 154 (Figure 6a). A good correspondence was found in the case of the Drávaszabolcs data among measurement dates. Our measurements showed a finer mean d_{60} mm than former data. Mean values were 0.5 mm in 2003 and 2012, while our measurement revealed a mean d_{60} value of 0.39 mm. Downstream of Barcs, the gravel fraction almost entirely disappeared and coarse sand prevailed in each monitored cross-section.

Due to the transitional character of the channel morphology sand fraction was present in almost the entire reach of interest. However, likely, armouring obscured the fraction in the upstream segment of the reach. Textural heterogeneity especially prevailed in meanders, where sand regularly appeared in the inner part of the curvatures. Deposition of suspended load was also typical on the sandbars of the inflection transects. Coarse gravel prevailed in the channel upstream of rkm 190, while the mixture of coarse and medium gravel was found between rkms 190 and 172. Downstream of rkm 170 fine gravel and sand dominated the channel. The rather abrupt change in the texture of the bedload is verified by the sudden drop in the channel slope at 175 km from the mouth. This change in riverbed gradient was verified by former sonar measurements (Halmai et al., 2020) performed in May 2019.
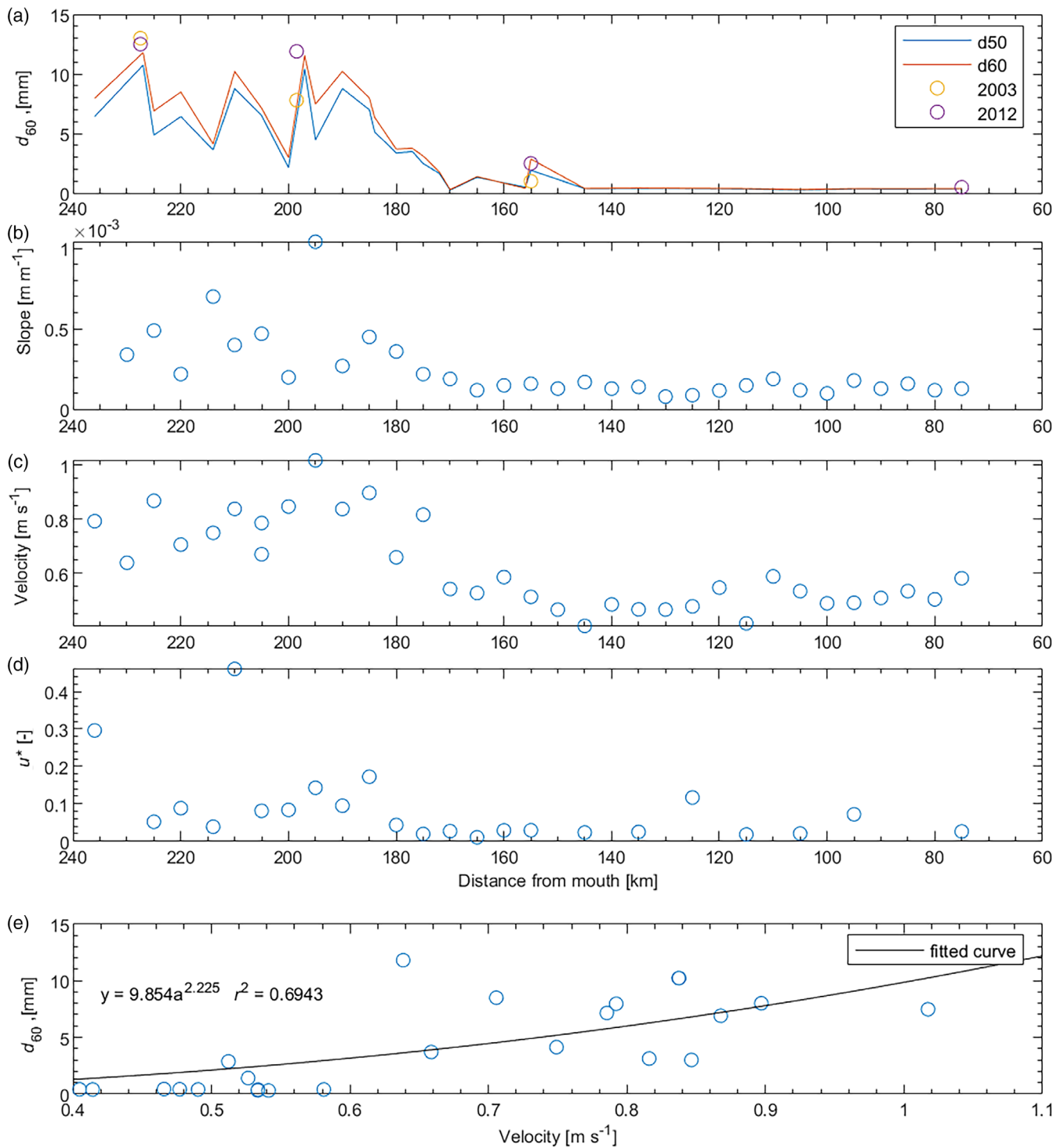
FIGURE 6 Longitudinal profile of (a) d_{60} bedload diameters with the corresponding 2003 and 2012 archive d_{60} diameters, (b) water surface slope, (c) flow velocities, (d) shear velocities and (e) d_{60} bedload diameters as a function of flow velocities in the Drava River between rkms 236 and 75 [Color figure can be viewed at wileyonlinelibrary.com]

3.2 | Distribution of the ADCP-measured mean and bottom flow velocities

The ADCP-measured flow velocities greatly varied along the longitudinal profile of the river. Flow velocities did not decrease monotonously in downstream direction. Highest flow velocity values were observed in the cross-section at rkm 195, with an average value of 1.01 m/s, while the lowest was measured at rkm 145 at a mean velocity of 0.40 m/s (Figure 6c). An abrupt drop in flow velocity was observed between rkms 175 and 170. The

TABLE 1 Hydromorphological parameters of Drava channel reaches where cutoffs were made after 1920

Cutoff reach (rkm)	Riverbed gradient (m/m)	Channel width (m)	Static armored layer	Maximum particle size class (mm)	d_{50}
160–158	0.00024	255	+	8–16	0.423
157–155	0.00113	243	+	8–16	2.793
151–148	0.00053	240	+	2.8–4	1.075
146–144	0.00132	210	−	2–2.8	0.392
139–133	0.00038	212	+	4–8	0.411
109–108	0.00257	155	−	1–2	0.350
86–85	0.00257	213	−	1–2	0.357
77–75	0.00094	284	−	1–2	0.370
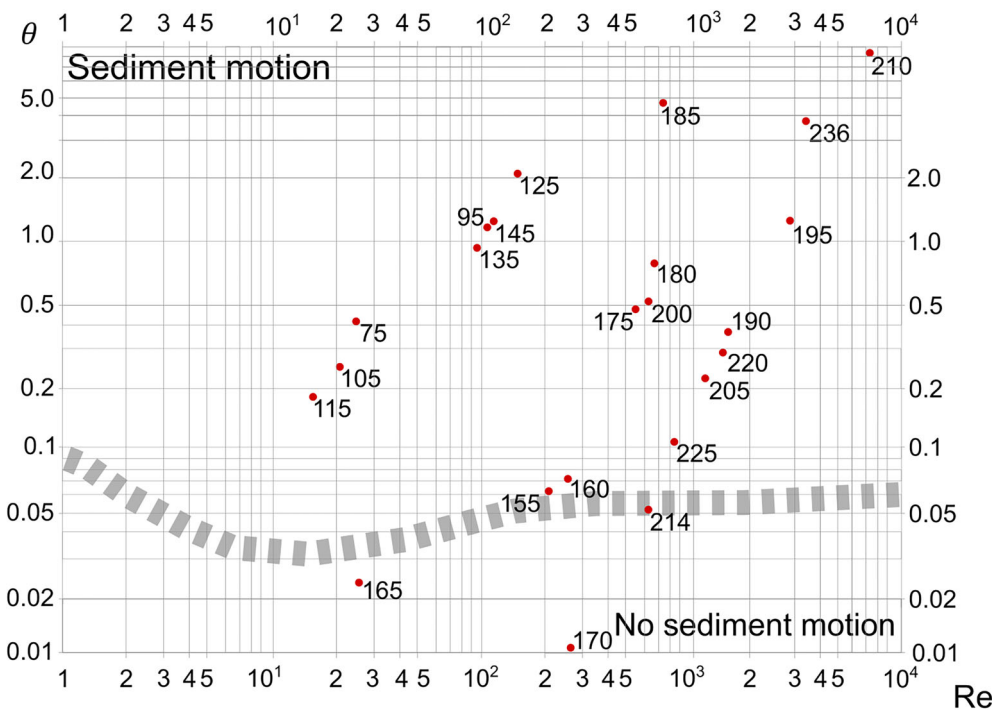
FIGURE 7 Calculated Shields numbers as a function of Reynolds numbers [Color figure can be viewed at wileyonlinelibrary.com]

location of this abrupt drop slightly lags behind the drop in water surface slopes along the longitudinal profile, that is, it is located at around rkms 195 to 180 (Figure 6b). Shear velocities showed a more heterogeneous picture, however, a local maximum is observed between rkm 200 and 185, followed by an abrupt decrease by rkm 180. Two additional shear velocity maxima were found at rkms 125 and 95, indicating complex flow dynamic on these reaches (Figure 6d). A power relation and a medium-strong correlation ($r^2 = 0.6943$) was found between d_{60} and the mean flow velocities for the studied transects (Figure 6e).

Bottom velocities (u_0) were typically 20–30% of the mean velocities and were generally less than 0.5 m/s. Commonly, noise in the velocity curves was higher for the mean velocity values than for the bottom velocities, caused by the turbulent character of the flow at closer to the water surface.

3.3 | Comparison of the estimated and calculated shear velocities

Shield numbers in almost all cross-sections were higher than the threshold Reynolds numbers indicating incipient sediment motion and entrainment of bed material (Figure 7). Entrainment rate was also affected by particle size. Deposition only prevailed between rkm 175 and 170, while hydraulic conditions were around the threshold values at rkm 214. Entrainment was minimal around rkms 160 and 155, where Shields number just barely exceeded the threshold (Figure 7). The reach between rkms 170 and 150 is located at the lower section of the abrupt drop in the longitudinal profile of flow velocities.

Significant differences were observed between the estimated and calculated shear velocities and Shields numbers. The estimated values

TABLE 2 Comparison of calculated and estimated shear velocities, Reynolds and Shields numbers

Cross-section (rkm)	Calculated			Estimated		
	$u*$	Re	θ	$u*$	Re	θ
225	0.0519	186.15	0.0461	0.1211	434.27	0.2507
165	0.0104	3.76	0.0184	0.0686	24.76	0.7969
115	0.0178	6.35	0.0548	0.0810	28.81	1.1289
105	0.0204	7.06	0.0733	0.0529	18.33	0.4943
75	0.0259	9.52	0.1115	0.0714	26.28	0.8488

were 2.5, in extreme cases 4 to sixfold, higher on average than the calculated values (Table 2). Shield numbers in almost all the selected cross-sections were above threshold Reynolds numbers indicating entrainment of bed material.

4 | CONCLUSIONS

For river management, to maintain navigational routes, the understanding of riverbed morphology and dynamics is indispensable. The present study was aimed at filling the research gap concerning sediment transport along the Lower Drava providing detailed additional data on bedload dynamics and textural distribution.

We validated the general downstream fining of bedload in the Drava River. However, the actual picture is more complex as the observed sediment pattern is rather heterogeneous and mosaic. We identified with higher precision than provided by Tamás (2019) the transitional section where abrupt sediment fining occurs. Our textural dataset for an average cross-section interval of 5.55 km presented a significant improvement and upgrade compared to the former point source data of five cross-sections over the entire studied reach.

Our findings revealed a fining of the bedload material over time in the Botovo (rkm 227) and Bélavár (rkm 198.5) transects compared to the 2003 and 2012 textural data. This fining can be explained by multiple factors.

1. The impact of climate change and decreasing flow rates by today, formerly pointed out by Bonacci and Oskoruš (2010), has significantly reduced river competence. The geomorphological interpretation of bedload transport and riverbed armouring underlines the long-term impact of river regulation, that is, meander cutoffs.
2. Armouring has been weakened by enhanced daily fluctuation induced hydropeaking. Incision of the river probably generated flow velocities higher than recorded by former measurements. Hydraulic sorting was observed, that is, increased differences among the transport of the individual fractions (in the sense of Paola & Seal, 1995). In contrast to the findings of Tamás (2019), demonstrated by the above threshold Reynolds and Shields numbers, the predominance of the entrainment of fine fractions was observed at many cross-sections of the studied reach (see Figure 7).
3. The measured textural composition of bedload has also been influenced by the variability of sampling points at cross-sections.

Bedload texture was averaged for cross-sections. Due to difficulties in keeping the vessel steady, sampling could not reflect cross-sectional changes in the transport field as sampling points could not be positioned at the same distance from the thalweg. This was the reason for some variations in the recorded textural composition.

4. The technical implementation of sampling slightly differed among the sampling dates and this fact makes comparisons more difficult. Specifically, the finer mesh size of the previously used bedload sampler may also contribute to the bias toward fine particles.

The hydraulic complexity of the river is underpinned by former hydromorphological analyses inasmuch as the rkm 235–185 reach of the Lower Drava has a pattern typical of the rivers of the Eastern Alpine Foreland: "transitional anabranching from the highly dynamic partially braided upstream reach to the meandering downstream part" (Schwarz, 2019).

Further field measurements will also enable the development of a functional relationship between hydromorphological parameters and bedload texture, which supports the understanding of future hydromorphological dynamics, and indirectly their ecological impacts. Although modern data acquisition methods based on Digital Elevation Model enable low-budget but high-resolution monitoring campaigns in multiple fields (geodesy, hydraulics, etc.), their application may substitute the costly, and often hazardous direct monitoring procedures but still presents challenges. Our findings may be relevant for the alluvial sections of other alpine and subalpine, partially channelized rivers of similar size, morphodynamics and mixed bedload too.

DATA AVAILABILITY STATEMENT

The data that support the findings of this study are available from the corresponding author upon reasonable request.

ORCID

Johanna Ficsor https://orcid.org/0000-0001-9439-516X
Dénes Lóczy https://orcid.org/0000-0002-2542-6775

REFERENCES

Ancey, C. (2020). Bedload transport: A walk between randomness and determinism. Part 1. The state of the art. *Journal of Hydraulic Research*, *58*(1), 1–17. https://doi.org/10.1080/00221686.2019.1702594

Ancey, C., Davison, A. C., Böhm, T., Jodeau, M., & Frey, P. (2008). Entrainment and motion of coarse particles in a shallow water stream down a steep slope. *Journal of Fluid Mechanics*, *595*, 83–114. https://doi.org/10.1017/S0022112007008774

Ashworth, P. J., & Ferguson, R. I. (1989). Size-selective entrainment of bed load in gravel bed streams. *Water Resources Research*, *25*(4), 627–634. https://doi.org/10.1029/WR025i004p00627

Bathurst, J. C. (2007). Effect of coarse surface layer on bedload transport. *Journal of Hydraulic Engineering*, *133*(11), 1192–1205. https://doi.org/10.1061/(ASCE)0733-9429(2007)133:11(1192)

Bialik, R. J., Nikora, V., Karpiński, M., & Rowiński, P. M. (2015). Diffusion of bedload particles in open-channel flows: Distribution of travel times and second-order statistics of particle trajectories. *Environmental Fluid Mechanics*, *15*(6), 1281–1292. https://doi.org/10.1007/s10652-015-9420-5

Bonacci, O., & Oskoruš, D. (2010). The changes in the lower Drava River water level, discharge and suspended sediment regime. *Environmental Earth Sciences*, *59*(8), 1661–1670. https://doi.org/10.1007/s12665-009-0148-8

Bonacci, O., Tadić, Z., & Trninić, D. (1992). Effects of dams and reservoirs on the hydrological characteristics of the lower Drava River. *Regulated Rivers: Research & Management*, *7*, 349–357.

Bunte, K., Abt, S. R., Swingle, K. W., & Potyondy, J. P. (2010). Functions to adjust transport rates from a Helley–Smith sampler to bedload traps in coarse gravel-bed streams (rating curve approach). In *2nd joint federal interagency conference, Las Vegas, NV, June 27–July 1, 2010*. 12 p. Advisory Committee on Water Information. Retrieved from https://acwi.gov/sos/pubs/2ndJFIC/Contents/10D_Bunte_03_01_10.pdf

Charru, F., Mouilleron, H., & Eiff, O. (2004). Erosion and deposition of particles on a bed sheared by a viscous flow. *Journal of Fluid Mechanics*, *519*, 55–80.

Chen, C.-L. (1991). Unified theory on power laws for flow resistance. *Journal of Hydraulic Engineering*, *117*, 371–389. https://doi.org/10.1061/(ASCE)0733-9429(1991)117:3(371)

Einstein, H. A. (1950). The bed-load function for sediment transportation in open channel flows. *Technical Bulletin*, *1026*, 1–71.

Emmett, W. W. (2010). Observations of bedload behavior in rivers and their implications for indirect methods of bedload measurement. *U.S. Geological Survey Scientific Investigations Report*, *5091*, 159–170.

Evans, E. G., & Wilcox, A. C. (2014). Fine sediment infiltration dynamics in a gravel-bed river following a sediment pulse. *River Research and Applications*, *30*(3), 372–384. https://doi.org/10.1002/rra.2647

Ferdowsi, B., Ortiz, C. P., Houssais, M., & Jerolmack, D. J. (2017). River-bed armouring as a granular segregation phenomenon. *Nature Communications*, *8*, 1363. https://doi.org/10.1038/s41467-017-01681-3

Furbish, D., Ball, A., & Schmeeckle, M. (2012). A probabilistic description of the bed load sediment flux: 4. Fickian diffusion at low transport rates. *Journal of Geophysical Research*, *117*, F03034. https://doi.org/10.1029/2012JF002356

Habersack, H., Jäger, E., & Hauer, C. (2013). The status of the Danube River sediment regime and morphology as a basis for future basin management. *International Journal of River Basin Management*, *11*(2), 153–166. https://doi.org/10.1080/15715124.2013.815191

Habersack, H., Nachtnebel, H. P., & Laronne, J. (2001). The continuous measurement of bedload discharge in a large alpine gravel bed river. *Journal of Hydraulic Research*, *39*(2), 125–133. https://doi.org/10.1080/00221680109499813

Halmai, Á., Gradwohl-Valkay, A., Czigány, S., Ficsor, J., Liptay, Z. Á., Kiss, K., ... Pirkhoffer, E. (2020). Applicability of recreational-grade interferometric sonar for the bathymetric survey and monitoring of the Drava River. *International Journal of Geo-Information*, *9*(3), 149–170. https://doi.org/10.3390/ijgi9030149

Hicks, D. M., & Gomez, B. (2016). Sediment transport. In G. M. Kondolf & H. Piégay (Eds.), *Tools in geomorphology* (2nd ed., pp. 324–356). Chichester, England: John Wiley and Sons. https://doi.org/10.1002/9781118648551.ch15

Holmes, R. R. (2010). Measurement of bedload transport in sand-bed rivers: A look at two indirect sampling methods. *U.S. Geological Survey Scientific Investigations Report*, *5091*, 236–252.

Kiss, T., & Andrási, G. (2019). Evolution of the Drava floodplain in Hungary in the last 100 years. In D. Lóczy (Ed.), *The Drava River: Environmental problems and solutions* (pp. 157–175). Cham, Switzerland: Springer International. https://doi.org/10.1007/978-3-319-92816-6_11

Lóczy, D., Dezső, J., & Gyenizse, P. (2017). Climate change in the eastern Alps and the flood pattern of the Drava River. *Ekonomska i Ekohistorija (Koprivnica)*, *13*, 5–13.

López, R., Vericat, D., & Batalla, R. J. (2015). Assessment of bed load transport formula for an armoured gravel-Bed River. *Tecnología y Ciencias del Agua*, *6*(2), 5–20.

Lovász, G. (1974). *Délkelet-Dunántúl geológiája és felszínfejlődése [Geological and morphological evolution of the south-eastern Transdanubia]*. Pécs, Hungary: Baranya Megyei Levéltár.

Murphy, J., Jones, J., Arnold, A., Duerdoth, C. P., Pretty, J. L., Naden, P. S., ... Collins, A. (2017). Can macroinvertebrate biological traits indicate fine-grained sediment conditions in streams? *River Research and Applications*, *33*(10), 1606–1617. https://doi.org/10.1002/rra.3194

Nikora, V., Habersack, H., Huber, T., & McEwan, I. (2002). On bed particle diffusion in gravel bed flows under weak bed load transport. *Water Resources Research*, *38*(6), 17-1-17-9. https://doi.org/10.1029/2001WR000513

Nikuradse, J. (1933). Stromungsgesetz in rauhen Rohren. *Verein Deutscher Ingenieure: Forschungsheft*, *361*, 1–22.

Owens, P. N., Batalla, R. J., Collins, A., Gomez, B., Hicks, M., Horowitz, A. J., ... Trustrum, N. (2005). Fine-grained sediment in river systems: Environmental significance and management issues. *River Research and Applications*, *27*(1), 696–717. https://doi.org/10.1002/rra.878

Paola, C., & Seal, R. (1995). Grain size patchiness as a cause of selective deposition and downstream fining. *Water Resources Research*, *31*(5), 1395–1407. https://doi.org/10.1029/94WR02975

Petrić, H., Tamás, E., & Lóczy, D. (2019). Flood history and river regulation. In D. Lóczy (Ed.), *The Drava River: Environmental problems and solutions* (pp. 105–124). Cham, Switzerland: Springer International. https://doi.org/10.1007/978-3-319-92816-6_8

Petts, G. E., & Wood, R. (1988). *Regulated rivers, research and management: River regulation in the United Kingdom*. Chichester, England: John Wiley and Sons.

Pitlick, J., Mueller, E. R., Segura, C., Cress, R., & Torizzo, M. (2008). Relation between flow, surface-layer armoring and sediment transport in gravel-bed rivers. *Earth Surface Processes and Landforms*, *33*(8), 1192–1209. https://doi.org/10.1002/esp.1607

Prettenthaler, F., & Dalla-Via, A. (Eds.). (2007). *Wasser & Wirtschaft im Klimawandel. Konkrete Ergebnisse am Beispiel der sensiblen Region Oststeiermark [Water and economy during climate change. Results on the example of the sensitive region of western Styria]*. Wien, Austria: Verlag der Österreichischen Akademie der Wissenschaften, Institut für Stadt- und Regionalforschung Forschungsberichte, Band 31. Studien Zum Klimawandel in Österreich.

Purger, J. J. (Ed.). (2008). *Biodiversity studies along the Drava River*. Pécs, Hungary: University of Pécs.

Raymond Pralong, M., Turowski, J. M., Rickenmann, D., & Zappa, M. (2015). Climate change impacts on bedload transport in alpine drainage basins with hydropower exploitation. *Earth Surface Processes and Landforms*, *40*(12), 1587–1599. https://doi.org/10.1002/esp.3737

Recking, A., Liébault, F., Peteuil, C., & Jolimet, T. (2012). Testing several bed load transport equations with consideration of time scales. *Earth*

Surface Processes and Landforms, 37(7), 774–789. https://doi.org/10.1002/esp.3213

Rhoads, B. L. (2020). Sediment transport dynamics in rivers. In B. L. Rhoads (Ed.), *River dynamics: Geomorphology to support management* (pp. 97–133). Cambridge, England: Cambridge University Press. https://doi.org/10.1017/9781108164108

Schwarz, U. (2008). Hydromorphological inventory and map of the Drava and Mura rivers (IAD pilot study). *Large Rivers*, 18(1–2), 45–59. https://doi.org/10.1127/lr/18/2008/45

Schwarz, U. (2019). Hydromorphology of the lower Drava. In D. Lóczy (Ed.), *The Drava River: Environmental problems and solutions* (pp. 61–78). Cham, Switzerland: Springer International. https://doi.org/10.1007/978-3-319-92816-6_5

Sharma, A., Herrera-Granados, O., & Kumar, B. (2019). Bedload transport and temporal variation of non-uniform sediment in a seepage-affected alluvial channel. *Hydrological Sciences Journal*, 64(8), 1001–1012. https://doi.org/10.1080/02626667.2019.1615621

Simpson, M., & Oltmann, R. (1990). An acoustic Doppler discharge-measurement system. In *HY Div/ASCE, Hydraulic engineering proceedings 1990 national conference* (p. 903). San Diego, CA: Hydraulics Division of the American Society of Civil Engineers.

Słowik, M., Dezső, J., Marciniak, A., Tóth, G., & Kovács, J. (2018). Evolution of river platforms downstream of dams: Effect of dam constuction or earlier humaninduced changes? *Earth Surface Process and Landforms*, 43(10), 2045–2063. https://doi.org/10.1002/esp.4371

Szlávik, L., Sziebert, J., & Tamás, E. A. (2012). *A Dráva morfológiai monitoringja – Hordalékvizsgálat [Sediment analysis study under the project of Dráva morphological monitoring]* Reference research report. Baja, Hungary: Eötvös József Főiskola.

Tamás, E. A. (2019). Sediment transport of the Drava River. In D. Lóczy (Ed.), *The Drava River environmental problems and solutions* (pp. 91–103). Cham, Switzerland: Springer International. https://doi.org/10.1007/978-3-319-92816-6_7

Tamás, E. A., & Ficsor, J. (2018). Questions in the quantitative analysis of sediment load – Example of three major rivers in Hungary. *River Flow*, 40(5), 4023. https://doi.org/10.1051/e3sconf/20184004023

Teledyne. (2018). *Win river user's guide*. Poway, CA: Teledyne RD. Instrument.

Uherkovich, Á., & Nógrádi, S. (1997). *Platyphylax frauenfeldi* Brauer, 1857 (Trichoptera, Limnephilidae) in Hungary. *Braueria*, 24, 13–14.

van Rijn, L. (1984). Sediment transport, part I: Bed load transport. *Journal of Hydraulic Engineering*, 110, 1431–1456. https://doi.org/10.1061/(ASCE)0733-9429(1984)110:10(1431)

Vázquez-Tarrío, D., Fernández-Iglesias, E., Fernández García, M., & Marquínez, J. (2019). Quantifying the variability in flow competence and streambed mobility with water discharge in a gravel-Bed Channel: River Esva, NW Spain. *Water*, 11(12), 2662–2688. https://doi.org/10.3390/w11122662

Wan Mohtar, W. H. M., Junaidi, S. S., & Mukhlisin, M. (2016). Representative sediment sizes in predicting the bed-material load for nonuniform sediments. *International Journal of Sediment Research*, 31, 79–86.

Wilcock, P. R., & DeTemple, B. T. (2005). Persistence of armor layers in gravel-bed streams. *Geophysical Research Letters*, 32(8), L08402. https://doi.org/10.1029/2004GL021772